Noise Analysis of a Photoreceiver Using a P-I-N and GaAs HBT Distributed Amplifier Combination

Xizhen Tian, A. P. Freundorfer, *Member, IEEE*, and Langis Roy, *Member, IEEE*

***Abstract*—A noise analysis for a Common-Collector-Cascode traveling wave HBT preamplifier is developed. The photoreceiver, consisting of a P-I-N and GaAs HBT MMIC distributed amplifier, was implemented using Nortel's $f_T = 70$ GHz GaAs HBT process, is the first to have a P-I-N mounted on the MMIC chip. The P-I-N preamplifier, having a measured bandwidth of 22 GHz, displayed a measured average equivalent input noise current density of 24 pA/$\sqrt{\text{Hz}}$. Good agreement was obtained between the predicted and measured noise performance.**

***Index Terms*—Distributed amplifier, HBT, P-I-N, preamplifier.**

I. Introduction

GaAs HBT distributed amplifiers (DAs) are attractive for optical receiver applications due to the HBT device's excellent threshold voltage uniformity, the advantage of low-phase jitter properties [1], [2], the DA's inherently high bandwidth, as well as the integration possibility with InGaAs P-I-N diodes [3]. HBT distributed amplifiers with wide bandwidth performance have been demonstrated [2]–[5] in recent years. Encouraged by this trend, a noise analysis for the HBT Common-Collector-Cascode (CCC) preamplifier is developed.

Noise performance analysis for MESFET preamplifiers has been widely published [6]–[8]. However, a noise analysis for the HBT CCC traveling wave preamplifier, has not been previously done, and is the subject of this letter. An optical receiver employing a P-I-N diode and a GaAs HBT MMIC distributed preamplifier combination was constructed, using Nortel's GaAs HBT and InGaAs P-I-N photodiode process. The HBT Spice model used in this paper has been validated in high speed lightwave systems at Nortel. The HBT preamplifier's noise performance is predicted by this noise analysis.

II. Noise Analysis of the HBT DA

A simplified schematic of a HBT CCC preamplifier is shown in Fig. 1. The short transmission lines on the input line, which are equivalent to inductors, and the equivalent input capacitances of the HBT gain cell, form a transmission line with an impedance equal to $Z_{\pi b}$. The collector line is formed in a similar way and is terminated by impedance $Z_{\pi c}$. The preamplifier includes the following noise sources: noise from the base termination $Z_{\pi b}$, noise from the collector termination $Z_{\pi c}$, and noise from the HBT gain cell. The noise model of the HBT CCC gain cell can be transformed into a noiseless two-port network with two correlated voltage and current noise generators (e_{nc} and i_{nc}) connected at its input, which is more suitable for noise analysis of a preamplifier. The derivation of noise sources e_{nc} and i_{nc} can be carried out analytically following the noise network theory. Then, following the same analysis method as in [8] except for a different gain cell, the transimpedance of the preamplifier in the passband can be derived as

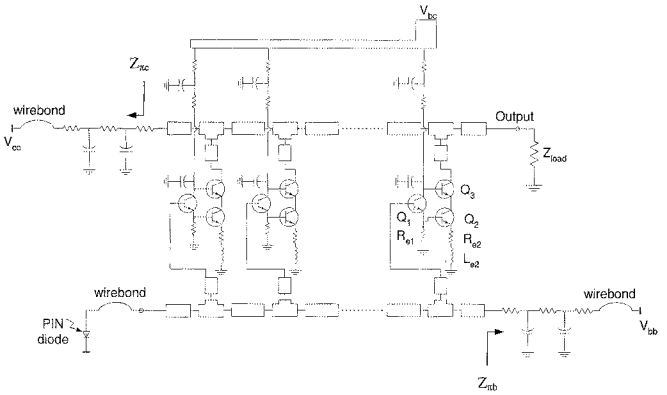

Fig. 1. Schematic of P-I-N HBT preamplifier.

$$Z_f = \frac{v_{out}}{i_s} = -\frac{1}{2} N \cdot G \cdot (Z_{\pi c} \cdot Z_{\pi b}) \cdot e^{-jN\phi} \tag{1}$$

where G is the equivalent transconductance of the HBT CCC, which is represented as the equation at the bottom of the next page and where g_m and r_b are the transconductance and base resistance of the HBT, respectively.

The equivalent input noise current density of the preamplifier is given by

$$\sqrt{|i_n|^2} = \sqrt{\begin{aligned} &\frac{|i_{Z\pi b}|^2}{4}\left|1+\frac{\sin N\phi}{N\sin\phi}\,e^{jN\phi}\right|^2 + \frac{|i_{Z\pi c}|^2}{4}\left|\frac{Z_{\pi c}}{Z_f}\right|^2 \\ &+\frac{|i_{nc}|^2}{4}\sum_{r=1}^{N}|C(r,\phi)|^2 + \frac{|e_{nc}|^2}{N}\left|\frac{1}{Z_{\pi b}}\right|^2 \\ &+\frac{1}{2}\sum_{r=1}^{N}\mathrm{Re}\left[i_{nc}e_{nc}^*\left(-\frac{2}{NZ_{\pi b}}\right)^* C(r,\phi)e^{j(-2r+1)\phi}\right] \end{aligned}} \tag{2}$$

Manuscript received August 3, 2002; revised November 20, 2002. The review of this letter was arranged by Associate Editor Dr. Arvind Sharma.

X. Tian is with Nortel Networks, Ottawa, ON K1Y 4H7, Canada.

A. P. Freundorfer is with the Department of Electrical and Computer Engineering, Queens University, Kingston, ON K7L 3N6, Canada.

L. Roy is with the Department of Electronics, Carleton University, Ottawa, ON K1S 5B6, Canada.

Digital Object Identifier 10.1109/LMWC.2003.814096

where

$$|i_{z\pi b}|^2 = \frac{4kt}{Z_{\pi b}} \quad \text{and} \quad |i_{z\pi c}|^2 = \frac{4kt}{Z_{\pi c}}$$

$$C(r,\phi) = 1 + \frac{(N-r+1)}{N} e^{j(2r-1)\phi} + \frac{1}{N}\frac{\sin(r-1)\phi}{\sin\phi} e^{j(r-1)\phi}$$

$$\overline{i_{nc}^2} = A_1 \left\{ \begin{array}{l} \overline{i_{11}^2}\,|g_{m1}R_{e1}|^2 + \overline{i_{12}^2}\,|Y_{\pi1}R_{e1}|^2 \\ \quad + \overline{i_{21}^2}\,|(R_{e1}+r_{b2}+R_{e2})Y_{\pi1}|^2 \\ \quad + \left(\overline{e_{e1}^2} + \overline{e_{b2}^2} + \overline{e_{e2}^2}\right)|Y_{\pi1}|^2 \end{array} \right\} + \left| \frac{1}{g_{m2}g_{m3}\,(Y_{\pi1}+g_{m1})\,R_{e1}} \right|^2 \cdot \left\{ \begin{array}{l} \overline{i_{22}^2}\,|(g_{m3}Y_{\pi1})\,[Y_{\pi2}(R_{e1}+R_{e2}) \\ \quad + (Y_{\pi2}r_{b2}+1)]|^2 \\ \quad + \overline{i_{31}^2}\,|g_{m3}C_1|^2 + \overline{i_{32}^2}\,|Y_{\pi3}C_1|^2 \end{array} \right\}$$

$$\overline{e_{nc}^2} = A_1 \left\{ \begin{array}{l} \overline{i_{11}^2}\,|R_{e1}\,(1-r_{b1}g_{m1})|^2 + \overline{i_{12}^2} \\ \quad \cdot |R_{e1}\,(Y_{\pi1}r_{b1}+1)|^2 \\ \quad + \overline{i_{21}^2}\,|A_0(r_{b2}+R_{e2}) \\ \quad + R_{e1}\,(Y_{\pi1}r_{b1}+1)|^2 \\ \quad + \overline{e_{b1}^2}\,|(Y_{\pi1}+g_{m1})R_{e1}|^2 \\ \quad + \overline{e_{e1}^2}\,|Y_{\pi1}r_{b1}+1|^2 + \left(\overline{e_{b2}^2}+\overline{e_{e2}^2}\right)|A_0|^2 \end{array} \right\} + \left| \frac{1}{g_{m2}g_{m3}\,(Y_{\pi1}+g_{m1})\,R_{e1}} \right|^2 \cdot \left\{ \begin{array}{l} \overline{i_{22}^2}\,|g_{m3}C_0 - g_{m2}g_{m3}R_{e2}A_0|^2 \\ \quad + \overline{i_{31}^2}\,|g_{m3}C_0|^2 + \overline{i_{32}^2}\,|Y_{\pi3}C_0|^2 \end{array} \right\}$$

$$i_{nc}e_{nc}^* = A_1 \left\{ \begin{array}{l} \overline{i_{11}^2}\,(g_{m1}R_{e1})\,[R_{e1}\,(1-r_{b1}g_{m1})]^* \\ \quad - \overline{i_{12}^2}\,(Y_{\pi1}R_{e1})\,[R_{e1}\,(Y_{\pi1}r_{b1}+1)]^* \\ \quad - \overline{i_{21}^2}\,[(R_{e1}+r_{b2}+R_{e2})\,Y_{\pi1}] \\ \quad \cdot [A_0(r_{b2}+R_{e2}) + R_{e1}\,(Y_{\pi1}r_{b1}+1)]^* \\ \quad - \overline{e_{e1}^2}Y_{\pi1}\,(Y_{\pi1}r_{b1}+1)^* - \overline{e_{b2}^2}Y_{\pi1}A_0^* \\ \quad - \overline{e_{e2}^2}Y_{\pi1}A_0^* \end{array} \right\} + \left| \frac{1}{g_{m2}g_{m3}\,(Y_{\pi1}+g_{m1})\,R_{e1}} \right|^2 \cdot \left\{ \begin{array}{l} -\overline{i_{22}^2}g_{m3}Y_{\pi1}\,[Y_{\pi2}\,(R_{e1}+R_{e2}) \\ \quad + (Y_{\pi2}r_{b2}+1)] \\ \quad \cdot [g_{m3}C_0 - g_{m2}g_{m3}R_{e2}A_0]^* \\ \quad + \overline{i_{31}^2}\,(g_{m3}C_1)\,(g_{m3}C_0)^* \\ \quad + \overline{i_{32}^2}\,(Y_{\pi3}C_1)\,(Y_{\pi3}C_0)^* \end{array} \right\}$$

$$C_0 = (Y_{\pi1}r_{b1}+1)\,Y_{\pi2}R_{e1} + [(Y_{\pi1}r_{b1}+1) + (Y_{\pi1}+g_{m1})R_{e1}] \cdot [(Y_{\pi2}r_{b2}+1) + (Y_{\pi2}+g_{m2})R_{e2}]$$

$$C_1 = Y_{\pi1} \cdot [Y_{\pi2}(R_{e1}+r_{b2}+R_{e2}) + 1 + g_{m2}R_{e2}]$$

$$A_0 = (Y_{\pi1}r_{b1}+1) + (Y_{\pi1}+g_{m1})\,R_{e1}$$

$$A_1 = \left| \frac{1}{(Y_{\pi1}+g_{m1})R_{e1}} \right|^2$$

$$Y_{\pi i} = \frac{1}{r_{\pi i}} + j\omega C_{\pi i}, \qquad i = 1,2,3.$$

where ϕ is the per stage phase delay of the distributed amplifier, and $r_{\pi i}$ and $C_{\pi i}$ are the HBT's model parameters. The first two terms in (2) are the noise densities produced by base termination $Z_{\pi b}$ and collector termination $Z_{\pi c}$, respectively. The remaining contributions are the noise sources produced by the HBT gain cells. $\overline{i_{nc}^2}$ and $\overline{e_{nc}^2}$ are the equivalent noise sources of the HBT gain cell, which are derived from the equivalent circuit of the HBT gain cell. $i_{nc}e_{nc}^*$ is the correlation between those two noise sources. i_{i1} and i_{i2} represent the input and output intrinsic current noise sources of transistor Q_i $(i = 1, 2, 3)$; e_{bi} is the thermal noise source due to the base resistor r_b of transistor Q_i. e_{e1} and e_{e2} are thermal noise sources due to resistor R_{e1} and R_{e2}. Inspecting (1) and (2), we can see that increasing $Z_{\pi b}$ will decrease the first, second, fourth and fifth terms of $|i_n|^2$. Therefore, the equivalent input noise current density of a HBT preamplifier can be reduced by increasing $Z_{\pi b}$. The effect of increasing $Z_{\pi b}$ is twofold: it increases the transimpedance gain Z_f. At same time, it reduces the magnitude of the equivalent noise current density. However, increasing $Z_{\pi b}$ will lead to a lower cutoff frequency of the input distributed structure, which will limit the bandwidth of the distributed amplifier. Fig. 2 shows simulated HBT preamplifier's equivalent input noise current density curves for $Z_{\pi b} = 60\ \Omega$ and $Z_{\pi b} = 40\ \Omega$, which confirms the improvement by increasing $Z_{\pi b}$. Our analysis also shows that the noise contribution of $Z_{\pi b}$ dominates the DA's equivalent input noise current density at low frequency, while the gain cell's noise contribution dominates at high frequency. $Z_{\pi c}$'s noise contribution is relatively small. In order to improve high frequency noise performance, the noise source of the gain cell should be reduced. This can be achieved by reducing the bias current of the HBTs.

III. Results

A monolithic eight-stage GaAs HBT distributed preamplifier was designed and fabricated. The DA chip was implemented using Nortel's GaAs HBT ($f_T = 70$ GHz) process in a CPW regime with $Z_{\pi b} = 60\ \Omega$, $Z_{\pi c} = 50\ \Omega$. Five HBT transistors were used to build one DA cell: a $2 \times 2\ \mu\text{m}^2$ HBT ($g_m = 55$ mS) for the CC (Common Collector) stage, and two pairs of 3×6.5

$$G = \frac{g_{m2}g_{m3}}{(Y_{\pi3}+g_{m3})} \cdot \frac{(Y_{\pi1}+g_{m1})R_{e1}}{(Y_{\pi1}r_{b1}+1)Y_{\pi2}R_{e1} + [(Y_{\pi1}r_{b1}+1)+(Y_{\pi1}+g_{m1})R_{e1}][(Y_{\pi2}r_{b2}+1)+(Y_{\pi2}+g_{m2})R_{e2}]}$$

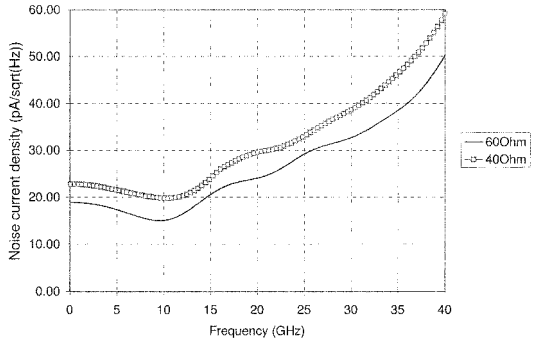

Fig. 2. HBT preamplifier's input equivalent noise current density versus input termination.

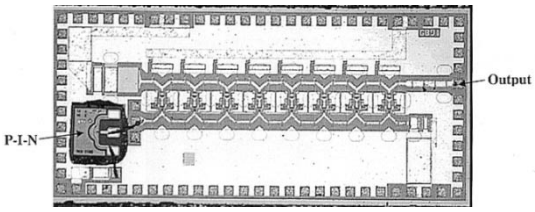

Fig. 3. Micro photograph of P-I-N, HBT distributed amplifier MMIC combination.

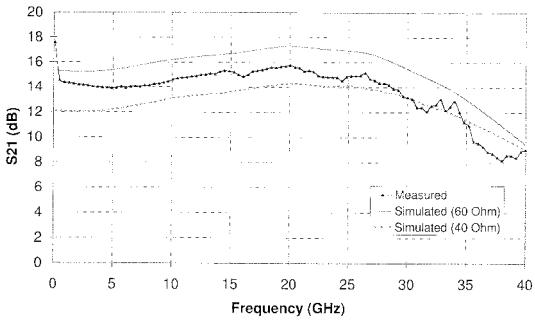

Fig. 4. Measured versus simulated S21 parameter of the HBT distributed amplifier.

μm^2 HBT ($g_m = 225$ mS) for the cascode. In order to optimize the complete photoreceiver's performance, the HBT distributed amplifier MMIC chip was designed to have a P-I-N mounted on it and connected to its input directly at the chip level, through a very short wire bond. The preamplifier's performance was optimized while the electrical model of the P-I-N and wire bond was integrated into the circuit during simulation.

Fig. 3 shows a micro photograph of the fabricated HBT preamplifier MMIC chip with the P-I-N mounted on it and wire bonded to its input. The measured optical response of the HBT P-I-N preamplifier showed a low frequency (<4 GHz) gain drop due to the absence of off-chip decoupling caps on DC bias lines and a 3 dB bandwidth of about 22 GHz, which is mainly limited by the P-I-N photodiode's bandwidth. This is confirmed by Fig. 4, showing the bandwidth of the fabricated HBT DA to be much wider (about 35 GHz). Fig. 4 also shows the impact of changing $Z_{\pi b}$ from 60 Ω to 40 Ω. The Nortel InGaAs P-I-N photodiode employed has a limited bandwidth due to its conventional vertically illuminated photodetector (VPD) structure [9]. Fig. 5 shows both the measured and analyzed equivalent input noise current density, as well as

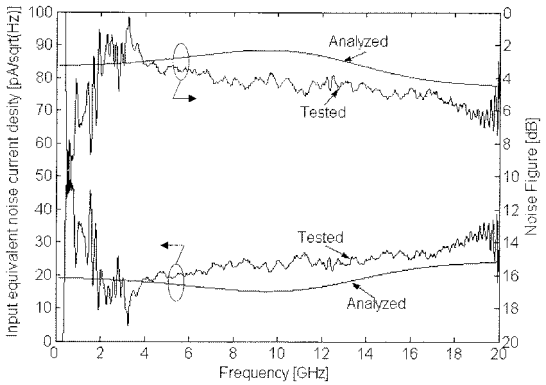

Fig. 5. Measured versus analyzed equivalent input noise current density and noise figure of the distributed preamplifier.

the corresponding noise figure, of the preamplifier up to 20 GHz. An average equivalent input noise current density of 24 pA/$\sqrt{\text{Hz}}$ was measured in the frequency range of 2–20 GHz. At lower frequencies (below 2 GHz), the measured noise appears much higher than expected due to the test setup, which allowed interfering radio frequency signals to be coupled into the circuit. It seems that the agreement between (2) and the measurement results is very good, hereby confirming the validity of the noise analysis.

IV. Conclusion

A noise analysis for the HBT CCC distributed preamplifier has been presented, resulting in an expression for the preamplifier's equivalent input noise current density. An implemented HBT distributed preamplifier has demonstrated a 3 dB bandwidth of 22 GHz and an average equivalent input noise current density of 24 pA/$\sqrt{\text{Hz}}$, which agrees well with analytical predictions. The analysis gives useful insight into the dominant noise contributions of the preamplifier.

References

[1] M. E. Kim *et al.*, "GaAs heterojunction bipolar transistor device and IC technology for high-performance analog and microwave applications," *IEEE Trans. Microwave Theory Tech.*, vol. 37, pp. 1286–1303, Sept. 1989.

[2] K. W. Kobayashi *et al.*, "A 50-MHz–55GHz multidecade InP-based HBT distributed amplifier," *IEEE Microwave Guided Wave Lett.*, vol. 7, pp. 353–355, Oct. 1997.

[3] S. Mohammadi, J.-W. Park, D. Pavlidis, J.-L. Guyaux, and J. C. Garcia, "Design optimization and characterization of high-gain GaInP/GaAs HBT distributed amplifiers for high-bit-rate telecommunication," *IEEE Trans. Microwave Theory Tech.*, vol. 48, pp. 1038–1044, June 2000.

[4] K. W. Kobayashi *et al.*, "Extending the bandwidth performance of heterojunction bipolar transistor-based distributed amplifiers," *IEEE Trans. Microwave Theory Tech.*, vol. 44, pp. 739–747, May 1996.

[5] Y. Baeyens, R. Pullela, J. P. Mattia, H.-S. Tsai, and Y.-K. Chen, "A 74-GHz bandwidth InAlAs/InGaAs-InP HBT distributed amplifier with 13-dB gain," *IEEE Microwave Guided Wave Lett.*, vol. 9, pp. 461–463, Nov. 1999.

[6] C. S. Aitchison, "The predicted signal to noise performance of a photodiode-distributed amplifier optical detector," in *IEEE MTT-S Dig.*, vol. 20, June 1992, pp. 769–772.

[7] J. Y. Liang and C. S. Aitchison, "Signal-to-noise performance of the optical receiver using a distributed amplifier and P-I-N photodiode combination," *IEEE Trans. Microwave Theory Tech.*, vol. 43, pp. 2342–2350, Sept. 1995.

[8] A. P. Freundorfer and T. L. Nguyen, "Noise in distributed MESFET preamplifier," *IEEE J. Solid-State Circuits*, vol. 31, pp. 1100–1111, Aug. 1996.

[9] K. Kato, "Ultrawide-band/high-frequency photodetectors," *IEEE Trans. Microwave Theory Tech.*, vol. 47, pp. 1265–1281, July 1999.